Supramolecular Chemistry in Molten Sulfur: Preorganization Effects Leading to Marked Enhancement of Carbon Nitride Photoelectrochemistry

*Jingsan Xu, Shaowen Cao, Thomas Brenner, Xiaofei Yang, Jiaguo Yu, Markus Antonietti, and Menny Shalom**

Here, a new method for enhancing the photoelectrochemical properties of carbon nitride thin films by in situ supramolecular-driven preorganization of phenyl-contained monomers in molten sulfur is reported. A detailed analysis of the chemical and photophysical properties suggests that the molten sulfur can texture the growth and induce more effective integration of phenyl groups into the carbon nitride electrodes, resulting in extended light absorption alongside with improved conductivity and better charge transfer. Furthermore, photophysical measurements indicate the formation of sub-bands in the optical bandgap which is beneficial for exciton splitting. Moreover, the new bands can mediate hole transfer to the electrolyte, thus improving the photooxidation activity. The utilization of high temperature solvent as the polymerization medium opens new opportunities for the significant improvement of carbon nitride films toward an efficient photoactive material for various applications.

1. Introduction

As a metal-free semiconductor, polymeric carbon nitride (simplified as CN) with its excellent stability against oxidation and corrosive chemical environments[1] has attracted growing attention, being a photo(electro)-catalyst for water splitting,[2] catalyst for organic syntheses,[3] or CO_2 capture and reduction.[4] Generally, CN is simply synthesized by thermal condensation of small organic molecules such as urea/thiourea, dicyandiamide, and melamine, which all contain properly connected carbon and nitrogen atoms.[5] However, the above techniques are solely able to obtain CN materials in their powder form.

Operation of catalysts in photoelectrochemistry (PEC) is an attractive alternative to convert solar energy to chemical fuels. The applications of CN in this field and other electronic devices (e.g., light-emitting diodes) are still in their infancy, and only few works were reported because of the difficulties in processing high-quality CN films with good adhesion and full coverage.[6] Due to the powder character of bulk CN and its poor solubility in most solvents, only inhomogeneous and weakly attached CN films could be obtained on functional substrates, using conventional deposition methods such as spin coating, drop casting, and screen printing. Given this situation, it is also difficult to improve and create new CN-like films, say using doping or introducing pores[7] that are frequently used to improve the potential of CN powders.[8]

Recently, we developed a liquid-mediated approach for the growth of uniform and continuous phenyl-modified carbon nitride (Ph-CN) thin films. In this method, a supramolecular-complex precursor fused to a liquid intermediate during heating, and finally condensed into a substituted carbon nitride that can be used as the electron–acceptor in organic solar cells[9] and emissive layer in organic light-emitting diodes.[10] However, the carbon nitride-like material still displays relatively low activity in photoelectronic devices due to insufficient charge transport properties. The reasons for the low charge mobility rely on the formation of grain boundaries and poor electrons/holes conductivity along the carbon nitride layer. One optional pathway to improve charge transport properties in CN-like materials is by the preorganization of CN monomers in a solvent via noncovalent bonding, such as hydrogen bond and π–π stacking.[11] The monomers preorganization allows one to create a continuous CN layer with the possibility to alter its chemical and photophysical properties.[12,13] Alongside the types of monomers, the solvent has a crucial role in the monomers preorganization due to its influence on the supramolecular interactions.[13] Hence, efforts are required on searching for suitable media from which the CN materials can be formed.

Dr. J. Xu, Dr. X. Yang, Prof. M. Antonietti, Dr. M. Shalom
Department of Colloid Chemistry
Max Planck Institute of Colloids and Interfaces
14424 Potsdam, Germany
E-mail: Menny.Shalom@mpikg.mpg.de
Prof. S. Cao, Prof. J. Yu
State Key Laboratory of Advanced Technology for Materials Synthesis and Processing
Wuhan University of Technology
Wuhan 430070, P.R. China
Dr. T. Brenner
Institute of Physics and Astronomy
University of Potsdam
14476 Potsdam, Germany

DOI: 10.1002/adfm.201502843

A unique "ancient" solvent is elemental sulfur.[14] The most stable allotrope is solid S_8 at ambient temperature, which melts at around 120 °C. It starts to polymerize into long chain polymeric sulfur at 159 °C and becomes very reactive when the temperature exceeds 250 °C.[15] The thermal transitions of S allow using sulfur as a high-temperature "reactive solvent" to prepare sulfur-contained composites for energy conversion and storage.[16] In addition, simulation by first-principle methods indicated that S-doped CN has a decreased overpotential and higher activity for the oxygen evolution reaction, as compared to a pure CN analog.[17] Inspired by these facts, we demonstrate here a co-melting strategy by combining molten sulfur and (supramolecularily aligned) liquid intermediates to in situ fabricate and modify phenyl-substituted carbon nitride (Ph-CN) thin films. Photophysical studies revealed that a sub-band is likely to occur from oriented phenyl subarrays within in the bandgap, which is able to trap photogenerated holes, and thus reduce charge recombination and promote hole transfer to the electrolyte. The sum of improved optical absorption, electronic conductivity, and hole transfer synergistically increased the photocurrent by a factor of 20 under visible light illumination with respect to the nonsulfur-processed analog.

2. Results and Discussion

2.1. Material Growth Studies

The growth of Ph-CN thin films on an FTO (fluorine-doped tin oxide) substrate follows our previous report[9] and is schematically shown in **Figure 1**. Briefly, cyanuric acid (CA) and 2,4-diamino-6-phenyl-1,3,5-triazine (Mp) were mixed in water in a 1:1 molar ratio to form a complex (noted as CMp). The CMp complex was mixed with different amount of sulfur and then transferred into a sealed crucible (Figure 1a). During heating, the sulfur melted first and served as a reactive dispersion agent. Throughout further heating to 400 °C, the solid CMp precursor turned liquid too and was able to form a homogenous mixture with the molten sulfur (Figure 1c). This description was backed by the in situ observation of the reaction mixture in a homemade, transparent setup (Figure S1a, Supporting Information). On the other hand, phase separation occurred for the mixture of sulfur and other nonphenylated precursors (Figure S1b, Supporting Information). We assume that the materials miscibility is due to the hydrophobic nature of sulfur which dissolved the phenyl groups in our special precursor to form stable micelles or microphases. FTO glass was placed under the precursor mixtures such that thermal polymerization of CN occurred on its surface. It is important to note that sulfur is completely

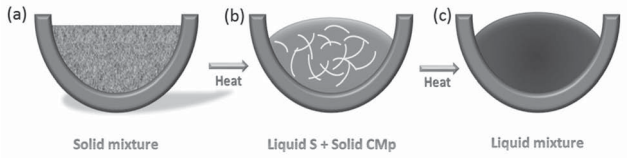

Figure 1. Scheme of the phase transitions of sulfur and CMp mixtures during heating: a) solid state mixture, b) molten S and solid CMp (curved lines), and c) liquid mixture of molten S and CMp.

evaporated at the final reaction temperature (500 °C) and therefore it is practically not incorporated within the CN structure. The sulfur-mediated CN is labeled as Ph-CNS_x representing a material made from the precursor of CMp mixed with *X* mg of sulfur.

Figure 2a shows the X-ray diffraction (XRD) patterns of the S-modified Ph-CN samples. The diffraction peak representing the interplanar stacking of connected tri-s-triazine at 27.5° shows a slight shift of 0.11° toward higher angle with sulfur (Figure S2, Supporting Information), indicating the stacking distance between two CN planes becomes smaller. The closer packing of the Ph-CN can be attributed to a better preorganization of the monomers, but strictly excludes the incorporation of sulfur within the planes. Due to the hydrophobic nature of sulfur, the monomers probably rearrange to create the most stable assembly in which the phenyl groups are in contact with the molten sulfur. Consequently, an organized microphase separated structure can be assumed to form during the heating process. The new rearrangement leads to better monomers packing and thus to shorter stacking distance between CN layers in the resulting product.

Elemental analysis shows that atomic carbon/nitrogen (C/N) ratio increases with the amount of S (Table S1, Supporting Information). We attribute the increase of the C/N ratio to the improvement of the phenyl group's incorporation into the Ph-CN networks. Fourier transform infrared spectroscopy (FTIR) spectra feature stretching bands of C-N heterocycles at 1200–1600 cm^{-1} and the vibration peak of triazine units at ≈810 cm^{-1}, further confirming the CN formation and demonstrating almost no changes for all the substrates (Figure S3, Supporting Information). The surface morphology of the Ph-CN thin films was studied with scanning electron microscope (SEM). The SEM pictures (Figure S4, Supporting Information) show homogeneous, porous CN films covering the FTO substrates, a morphology which is expected to promote the penetration of liquid electrolyte throughout the PEC operation. It is interesting to note that the surface morphology shows almost no changes even when 1200 mg of S was used throughout film processing, thus again underlining the sulfur practically does not contribute to the final film. The preservation of the crystal structure as well as morphology indicates that the improved photoactivity of the Ph-CN thin films should be ascribed to the modification of optical and electronic properties, as will be discussed later.

X-ray photoelectron spectroscopy (XPS) shows the evolution of chemical states of C, N, and S in the CN substrates. As displayed in Figure 2b, the reference Ph-CN substrate does expectedly not show any signal of S. A very weak peak (also concerning that sulfur is the heaviest element under examination) with the binding energy of 168.8 eV emerges when 100 mg of S was used, indicating the presence of very low amounts of surface bound of SO_4.[2–18] For Ph-CNS_{600}, a second S 2p-peak centered at 164.6 eV was observed, which is ascribed to the formation of C—S bonds, suggesting small amount of S atoms is connected to the Ph-CN framework.[19] The C 1s spectra of Ph-CN, Ph-CNS_{100}, and Ph-CNS_{600} substrates are shown in Figure 2c. The fitted C 1s curve of Ph-CN is displayed in Figure S5 (Supporting Information), and the peak at lower binding energy was deconvoluted into two peaks at 284.8 and 285.7 eV, which can

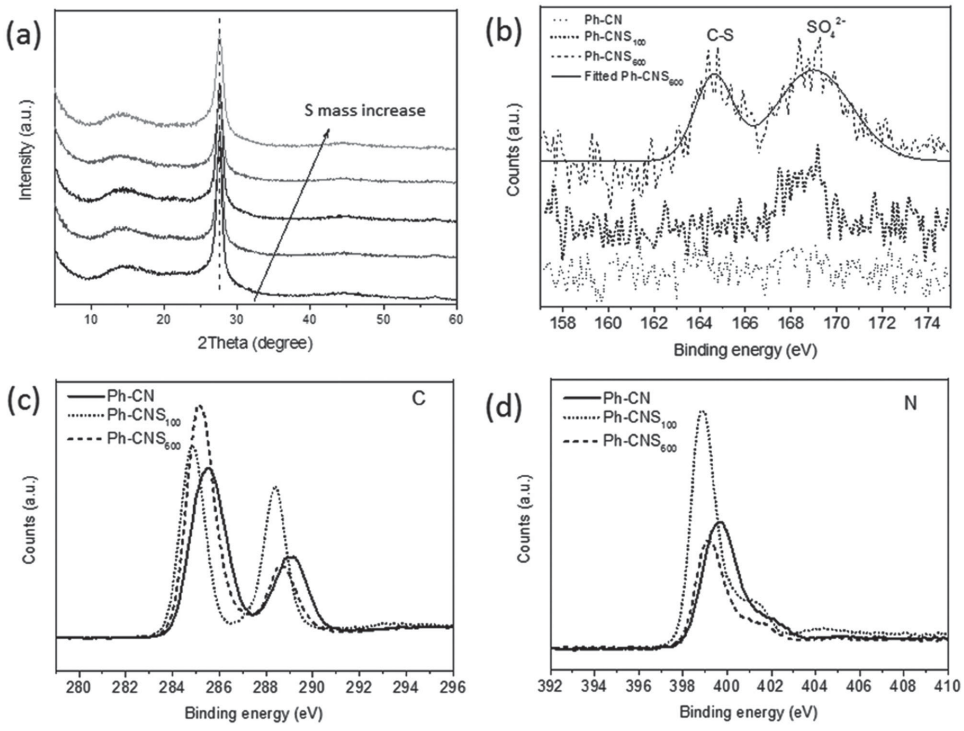

Figure 2. a) XRD patterns of CN substrates from bottom to top: Ph-CN, Ph-CNS_{100}, Ph-CNS_{400}, Ph-CNS_{600}, and Ph-CNS_{1200}. XPS spectrum: b) sulfur, c) carbon, and d) nitrogen of Ph-CN, Ph-CNS_{100}, and Ph-CNS_{600} substrate.

be assigned to C—C bonding from the phenyl group and C—O—C bonding originating from CA molecules, respectively. The other peak at higher binding energy was also deconvoluted into two peaks at 288.2 and 289 eV. The 288.2 eV one is a characteristic binding energy for C-$(N)_3$ coordination of the tri-s-triazine units. We assume the higher component (289 eV) is induced by the insertion of oxygen and consequent creation of $(N)_2$-C-O surface termination groups. This assumption can also be evidenced by the shift of N 1s peak (Figure 2d) to higher binding energy (399.7 eV) compared to the normally observed value (398.7 eV).[20]

In the case of Ph-CNS_{100}, the C 1s XPS spectrum shows a shift to lower binding energies, and the two peaks are solely attributed to C—C bonding of phenyl group (284.8 eV) and C-$(N)_3$ coordination (288.3 eV), respectively (Figure 2c). The intensity of the peak at 284.8 eV strongly indicates more efficient insertion of phenyl into the CN layers, which was already confirmed by the increased C/N ratio; and the shift can be explained by the removal of oxygen from the CN structures due to the reaction of S with oxygen species, which can be evidenced by the formation of SO_4^{2-} mentioned above. Interestingly, we notice that the C 1s binding energies for Ph-CNS_{600} substrate shift back to higher values which corresponds well with previous reports for CN materials.[21] We propose that this arises from the increase of structural perfection of Ph-CN, which is likely to be beneficial to the photoactivity of the electrodes. Comparing the absolute intensities of the C and N peaks with the sulfur and oxygen peaks, it is clear that sulfur remains within the structure only as surface defects or rare surface termination sites: its real role is a processing agent, also supporting copolymerization, but rather not a dopant, as described before for other sulfur containing monomers.[14,22]

2.2. Optical Properties and PEC Evaluations

Figure 3a shows the UV–vis absorption spectra of the CN substrates, demonstrating the enhancement of the optical absorption due to sulfur processing. We observe that absorption tails start to form (with energy levels at 500–600 nm) for low S mass (up to 100 mg). The absorption edge starts to present a red shift from 500 to 525 nm when 400 mg of S was used. Further shift to ≈600 and 650 nm occurs in the cases of higher S amount (600 and 1200 mg), indicating that the electronic structure and the band gap can be tuned by altering the amount of S present throughout synthesis, also reflected by the color changing of the substrates (inset of Figure 3a). On the basis of the characterization data, we interpret this effect as that high amounts of S induced more effective integration and enhanced stacking of phenyl into the CN framework, due to a more disperse starting situation. The preorganization of the phenyl groups creates a new charge transfer path in Ph-CN due to the interaction of the aromatic system with the electron-rich CN framework.

In order to further understand the effects of sulfur on the growth and modification of carbon nitride, intermediate products were acquired by heating the mixture of CMp and 600 mg S at lower temperatures (300 and 400 °C). S was molten at 300 °C and acted as a high-temperature solvent, while the CMp precursor was still in the solid state and did not undergo phase transition. In this scenario, the S solvent has almost no

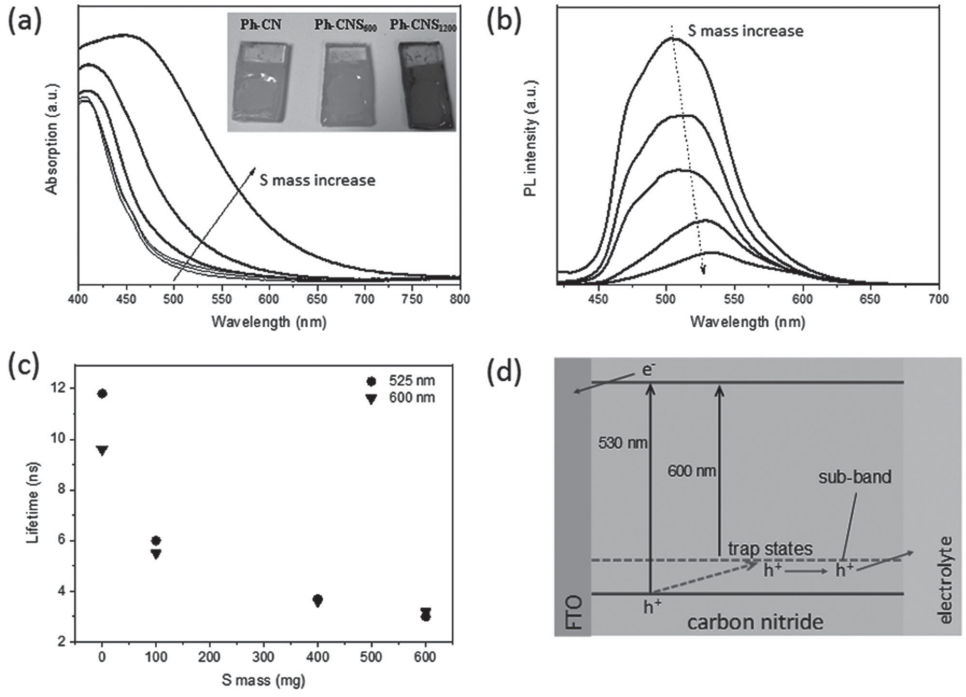

Figure 3. a) UV–vis absorption (inset, photograph of the substrates), b) PL spectra, and c) carrier lifetime of Ph-CN thin films with different S amount. d) Proposed band structure, charge generation, and charge transfer path of Ph-CNS_{600} substrate.

effect on the structure or bonding of the product, reflected by the XRD patterns and FTIR spectra (Figure S6a,c, Supporting Information). Nevertheless, UV–vis spectra suggest that the presence of sulfur altered the absorption of the product by introducing the absorption tails (Figure S6d, Supporting Information). At 400 °C, the CMp precursor turned to a graphitic structure after heating, as seen from the substantially evolved XRD patterns (Figure S6b, Supporting Information). Importantly, the absorption spectra of this sample showed that sulfur shifted the absorption edge of the material by up to 20 nm (Figure S6d, Supporting Information). From these experiments we concluded that the liquid phase of the CMp precursor is crucial for the creation of CMp dispersion in molten sulfur. Only afterward, the CMp monomers can reorganize to form the desired phenyl-modified carbon nitride film.

The optical properties of the Ph-CN thin films were further investigated by photoluminescence (PL; Figure 3b) under an excitation wavelength of 400 nm. The pristine Ph-CN substrate showed a strong PL emission centered at ≈515 nm while the use of low S amount (up to 100 mg) leads to PL quenching and no shift to lower energies (i.e., no shift in band–band transition), corresponding to the UV–vis spectra. The quenching is presumably due to the formation of defect states/surface states that promote a nonradiative charge carrier relaxation. It was demonstrated before that sulfur-mediated synthesis can enhance the absorption and photoactivity of CN materials[14] and in particular, Wang's group demonstrated that the sulfur flux can modify the thermal condensation route of melamine and tune the texture and electronic properties of the resulted CN powders.[22] Further PL intensity reduction was found for Ph-CNS_{400} and Ph-CNS_{600}, alongside with shifts of the fluorescence peak. We notice that for these two substrates a spectral shoulder at ≈600 nm can be distinguished, besides the central emission at ≈530 nm (Figure S7a, Supporting Information). We propose that the valence bands (VB) holes are shifting partly toward the sub-band states for materials with more than 400 mg of S, and mostly an emission around 600 nm is obtained. This trend is further developed in the PL spectrum of the Ph-CNS_{1200} material (Figure S7b, Supporting Information); despite the emission being highly quenched, a dual-peak signal (530 and 600 nm) can be clearly recognized and attributed to the CB-VB (conduction and valence band) and defect level transition, respectively. Time resolved photoluminescence measurements indicate the fluorescence lifetime decreases for the higher sulfur contents, typically from 11.8 ns for Ph-CN down to 3.0 ns for Ph-CNS_{600} monitored at 525 nm (which corresponds to the CB-VB emission) as shown in Figure 3c. This is due to new nonradiative paths for charge transfer being active in this few nanosecond region that can be considered to enhance the photo stability and thereby reactivity of electrons and hole within CN layers. Furthermore, we note the fluorescence lifetime of the Ph-CN substrate reasonably decreases to 9.6 ns when monitored at 600 nm (innerband transition level), while only slight change occurs for Ph-CNS_{400} (from 3.7 to 3.6 ns). For Ph-CNS_{600} an even longer lifetime is obtained (3.2 ns), as compared to that gained at 525 nm. This phenomenon strongly confirms the presence of new charge migration paths which might be employable for the photoelectrochemical activity. We suggest that the more effective integration of phenyl groups on the surface leads to the creation of subphases with well-placed sub-bands close to the valence band which act as acceptors for the photoexcited holes (Figure 3d) and might even be able to split the exciton to the two phases. These traps, as specially

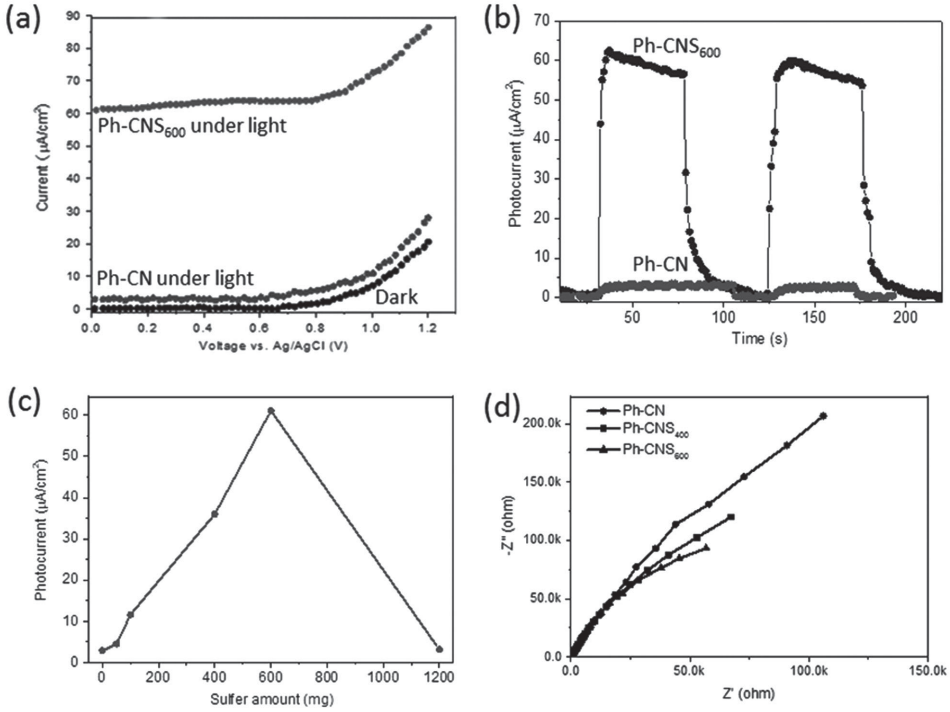

Figure 4. a) LSV curves of Ph-CN and Ph-CNS_{600} substrates in the dark and under illumination; b) current record with light "on" and "off" of Ph-CN and Ph-CNS_{600} substrates versus time with no applied voltage; c) S amount dependent photocurrent; and d) Nyquist curves of Ph-CN, Ph-CNS_{400}, and Ph-CNS_{600} substrate measured in the dark.

separated from the bulk, are able to inhibit the recombination of holes and electrons within the CN; as located at the surface, they also increase the holes' probability to react with the liquid phase species, which is beneficial for PEC activity.

PEC measurements in aqueous solution were performed to evaluate the effect of the sulfur synthesis on the photoactivity of Ph-CN substrates in 0.1 M KOH with a three-electrode system, using a Pt wire as the counter electrode and Ag/AgCl as the reference electrode. Linear sweep voltammetry scans (LSVs) recorded in the dark and under white light illumination show that all the Ph-CN substrates have a substantial photoresponse (bare FTO has no visible-light response). Typically, the LSV curves and the transient photocurrent studies under zero voltage from Ph-CN and Ph-CNS_{600} (**Figure 4**a,b) demonstrate that the Ph-CN substrate shows a saturated photocurrent of 2.9 μA cm^{-2}, while the Ph-CNS_{600} substrate shows a significantly enhanced photocurrent of ≈60 μA cm^{-2}. The photocurrents presented here are much higher than those obtained from deposition-processed CN electrodes (usually prepared by approaches such as drop casting).[23,24] The photocurrent for Ph-CNS_{600} slightly drops during illumination, presumably because of saturation of trap states and a consecutive slight increase of the recombination rate, while the Ph-CN substrate demonstrates quite stable current density under illumination probably due to the lower electron and hole concentrations.

The photoactivity of the Ph-CN substrates increases linearly with the amount of S added (up to 600 mg) while the performance is greatly retarded when too much sulfur was used (1200 mg), as shown in Figure 4c. This observation indicates that the change in light absorption is only partially responsible for the performance enhancement; there is also a strong electronic effect. Up to 600 mg of S, the defect levels can mediate the hole transfer from the VB to the electrolyte, while for higher S amount the defect levels overlap with the VB and the photogenerated holes have shorter life time which inhibits their chance to transfer to the electrolyte.

Another reason for the photoresponse enhancement is the increased conductivity of Ph-CN films. We employed electrochemical impedance spectroscopy (EIS) to analyze that contribution. As shown in Figure 4d, electronic conductivity in the dark of Ph-CNS_{400} and Ph-CNS_{600} compared to the pristine Ph-CN electrode is highly enhanced, as suggested by the compressed semicircles of the Nyquist curves. Such an improvement of conductivity with increased carbon content in the modified CN was shown before.[23] It is also worth mentioning that the Ph-CN films did not show any delamination of the active layer during and after any (photo)electrochemistry measurements.

3. Conclusion

In summary, we delineated an improved processing pathway for a phenyl-substituted CN photoelectrode by using sulfur as a high temperature reactive solvent to enhance organization and thermal polymerization. Detailed material characterization revealed that sulfur can texture the growth and lead to more effectively integrated phenyl groups into the thin films, resulting in extended light absorption and improved conductivity and charge transfer process. As a result, a significant enhancement of PEC activity was acquired, which was in

addition to these two effects due to the formation of subphases with sub-bands, which potentially help to split the excitons and mediate the hole transfer to the electrolyte. The unique liquidity of the intermediate states during the CN synthesis endows us in principle to introduce various other reactants (liquids and solids) for property modification. We believe that this work opens the path to manage and process carbon nitride thin films in a more controlled, robust way to improve optical and electronic properties toward more efficient carbon nitride based photoelectrochemical cells and devices.

4. Experimental Section

Substrates Fabrication: The growth of sulfur modified carbon nitride thin films on FTO (fluorine-doped tin oxide) glass was processed based on our previous report. All the chemicals were purchased from Sigma-Aldrich and used without further purification. Specifically, 1.30 g of CA and 1.80 g of Mp were weighed and mixed in 50 mL deionized water. The mixture was shaken overnight to form a milky CMp complex. Afterward the CMp powder was washed with water and separated by centrifugation at 5000 rpm. After drying at 60 °C in vacuum, different mass of sulfur (50–1200 mg) was weighed and mixed with the CMp by fine grinding in a mortar. Then the mixture of sulfur and the CMp precursor was transferred into a crucible, totally covering the FTO glass on the bottom. Afterward the crucible was capped and kept in an oven at 500 °C for 4 h under the protection of nitrogen atmosphere, with a heating rate of 2.3 °C min^{-1}. After cooling to room temperature the substrate was cleaned with sonication in water to remove the residual aggregates on the surface.

Photoelectrochemistry Measurements: The modified carbon nitride substrates were used as the working electrode in the typical three-electrode photoelectrochemical cell with a Gamry Reference 3000 potentiostat (Gamry Instruments). Linear sweep voltammetry (LSV) was performed at a scan rate of 20 mV s^{-1}. Photocurrent response under visible light irradiation was recorded at zero bias, using Pt wire as counter electrode, a saturated Ag/AgCl as reference electrode, and 0.1 M KOH aqueous solution as the electrolyte. A 50 W white LED ($\lambda > 410$ nm, HLN-60H-24A, Mean Well) was used as the light source without filters and the illumination intensity can be tuned. The light was chopped manually. EIS measurements were carried out in the same configuration cell.

Characterizations: XRD patterns were measured on a Bruker D8 Advance instrument using Cu-Kα radiation. Energy disperse X-ray analysis and morphology observation by scanning electron microscope (SEM) were performed on JSM-7500F (JEOL) equipped with an Oxford Instruments X-MAX80 mm^2 detector. FTIR spectra were recorded on a Nicolet iS5 FT-IR spectrometer (Thermal Scientific). Solid UV–vis absorbance spectra were measured using a UV-2600 spectrophotometer (Shimadzu, Japan) equipped with an integrating sphere. The emission spectra were recorded on LS-50B, Perkin Elmer instrument with the excitation wavelength of 400 nm. Elemental analysis of the powders (scratched from FTO substrates) was accomplished as combustion analysis using a Vario Micro device. XPS was investigated with ultrahigh vacuum VG EXCALAB 210 electron spectrometer using Mg K_α(1253.6 eV) as radiation source. Time-resolved fluorescence measurements were performed by using a time-correlated single photon counting setup with a Becker&Hickl SPC-130 acquisition system and a multichannel PML-16-C-1 PMT detector. Excitation at 475 nm was provided by a PicoQuant PDL-800B CW laser with a repetition rate of 2 MHz and emission was monitored at 525 and 600 nm.

Supporting Information

Supporting Information is available from the Wiley Online Library or from the author.

Acknowledgements

The authors would like to thank the technical staff at MPIKG and the "Nanojunction Design for Uphill Photosynthesis" group members.

Received: July 10, 2015
Revised: August 18, 2015
Published online: September 11, 2015

[1] a) X. Wang, K. Maeda, A. Thomas, K. Takanabe, G. Xin, J. M. Carlsson, K. Domen, M. Antonietti, *Nat. Mater.* **2009**, *8*, 76; b) Y. Wang, X. Wang, M. Antonietti, *Angew. Chem. Int. Ed.* **2012**, *51*, 68; c) X. Wang, S. Blechert, M. Antonietti, *ACS Catal.* **2012**, *2*, 1596; d) J. Zhang, Y. Chen, X. Wang, *Energy Environ. Sci.* **2015**, DOI: 10.1039/C5EEo1895A; e) J. Zhang, X. Wang, *Angew. Chem. Int. Ed.* **2015**, *54*, 7230.

[2] a) J. Zhang, M. Zhang, C. Yang, X. Wang, *Adv. Mater.* **2014**, *26*, 4121; b) T. Y. Ma, S. Dai, M. Jaroniec, S. Z. Qiao, *Angew. Chem. Int. Ed.* **2014**, *53*, 7281; c) Y. Zheng, Y. Jiao, Y. Zhu, L. H. Li, Y. Han, Y. Chen, A. Du, M. Jaroniec, S. Z. Qiao, *Nat. Commun.* **2014**, *5*, 3783. d) J. Wang, C. Zhang, Y. Shen, Z. Zhou, J. Yu, Y. Li, W. Wei, S. Liu, Y. Zhang, *J. Mater. Chem. A* **2015**, *3*, 5126.

[3] a) F. Su, S. C. Mathew, L. Möhlmann, M. Antonietti, X. Wang, S. Blechert, *Angew. Chem. Int. Ed.* **2011**, *50*, 657; b) P. Zhang, Y. Gong, H. Li, Z. Chen, Y. Wang, *RSC Adv.* **2013**, *3*, 5121.

[4] a) J. Yu, K. Wang, W. Xiao, B. Cheng, *Phys. Chem. Chem. Phys.* **2014**, *16*, 11492; b) P. Niu, Y. Yang, J. C. Yu, G. Liu, H.-M. Cheng, *Chem. Commun.* **2014**, *50*, 10837; c) J. Qin, S. Wang, H. Ren, Y. Hou, X. Wang, *Appl. Catal. B: Environ.* **2015**, *179*, 1; d) K. S. Lakhi, A. V. Baskar, J. M. Zaidi, S. S. Al-Deyab, M. El-Newehy, J. H. Choy, A. Vinu, *RSC Adv.* **2015**, *5*, 40183.

[5] Y. Gong, M. Li, Y. Wang, *ChemSusChem* **2015**, *8*, 931.

[6] a) J. Liu, H. Wang, Z. P. Chen, H. Moehwald, S. Fiechter, R. van de Krol, L. Wen, L. Jiang, M. Antonietti, *Adv. Mater.* **2015**, *27*, 712; b) J. Bian, J. Li, S. Kalytchuk, Y. Wang, Q. Li, T. C. Lau, T. A. Niehaus, A. L. Rogach, R.-Q. Zhang, *ChemPhysChem* **2015**, *16*, 954; c) J. Zhang, M. Zhang, L. Lin, X. Wang, *Angew. Chem. Int. Ed.* **2015**, *54*, 6297.

[7] a) J. Xu, T. J. K. Brenner, Z. Chen, D. Neher, M. Antonietti, M. Shalom, *ACS Appl. Mater. Interfaces* **2014**, *6*, 16481; b) S. Yan, Z. Li, Z. Zou, *Langmuir* **2010**, *26*, 3894; c) J. Zhang, G. Zhang, X. Chen, S. Lin, L. Möhlmann, G. Dołęga, G. Lipner, M. Antonietti, S. Blechert, X. Wang, *Angew. Chem. Int. Ed.* **2012**, *51*, 3183.

[8] a) X.-H. Li, X. Wang, M. Antonietti, *Chem. Sci.* **2012**, *3*, 2170; b) G. Zhang, X. Wang, *J. Catal.* **2013**, *307*, 246; c) J. Zhang, M. Zhang, S. Lin, X. Fu, X. Wang, *J. Catal.* **2014**, *310*, 24; d) Z. Lin, X. Wang, *Angew. Chem. Int. Ed.* **2013**, *52*, 1735.

[9] J. Xu, T. J. K. Brenner, L. Chabanne, D. Neher, M. Antonietti, M. Shalom, *J. Am. Chem. Soc.* **2014**, *136*, 13486.

[10] J. Xu, M. Shalom, F. Piersimoni, M. Antonietti, D. Neher, T. J. K. Brenner, *Adv. Opt. Mater.* **2015**, *3*, 913.

[11] a) Y. Liao, S. Zhu, J. Ma, Z. Sun, C. Yin, C. Zhu, X. Lou, D. Zhang, *ChemCatChem* **2014**, *6*, 3419; b) Y. S. Jun, E. Z. Lee, X. Wang, W. H. Hong, G. D. Stucky, A. Thomas, *Adv. Funct. Mater.* **2013**, *23*, 3661.

[12] Y.-S. Jun, J. Park, S. U. Lee, A. Thomas, W. H. Hong, G. D. Stucky, *Angew. Chem. Int. Ed.* **2013**, *52*, 11083.

[13] M. Shalom, S. Inal, C. Fettkenhauer, D. Neher, M. Antonietti, *J. Am. Chem. Soc.* **2013**, *135*, 7118.

[14] J. Zhang, J. Sun, K. Maeda, K. Domen, P. Liu, M. Antonietti, X. Fu, X. Wang, *Energy Environ. Sci.* **2011**, *4*, 675.

[15] B. Meyer, *Chem. Rev.* **1976**, *76*, 367.
[16] a) J. Wang, J. Yang, J. Xie, N. Xu, *Adv. Mater.* **2002**, *14*, 963; b) J. Fanous, M. Wegner, M. B. M. Spera, M. R. Buchmeiser, *J. Electrochem. Soc.* **2013**, *160*, A1169.
[17] S. Lin, X. Ye, X. Gao, J. Huang, *J. Mol. Catal. A: Chem.* **2015**, *406*, 137.
[18] G. Liu, P. Niu, C. Sun, S. C. Smith, Z. Chen, G. Q. Lu, H.-M. Cheng, *J. Am. Chem. Soc.* **2010**, *132*, 11642.
[19] S.-A. Wohlgemuth, R. J. White, M.-G. Willinger, M.-M. Titirici, M. Antonietti, *Green Chem.* **2012**, *14*, 1515.
[20] X. Yang, H. Tang, J. Xu, M. Antonietti, M. Shalom, *ChemSusChem* **2015**, *8*, 1350.
[21] a) L. Jia, H. Wang, D. Dhawale, C. Anand, M. A. Wahab, Q. Ji, K. Ariga, A. Vinu, *Chem. Commun.* **2014**, *50*, 5976; b) X. Zhang, H. Wang, H. Wang, Q. Zhang, J. Xie, Y. Tian, J. Wang, Y. Xie, *Adv. Mater.* **2014**, *26*, 4438.
[22] J. Zhang, M. Zhang, G. Zhang, X. Wang, *ACS Catal.* **2012**, *2*, 940.
[23] J. S. Zhang, X. F. Chen, K. Takanabe, K. Maeda, K. Domen, J. D. Epping, X. Z. Fu, M. Antonietti, X. C. Wang, *Angew. Chem. Int. Ed.* **2010**, *49*, 441.
[24] a) F. Dong, Z. Zhao, T. Xiong, Z. Ni, W. Zhang, Y. Sun, W.-K. Ho, *ACS Appl. Mat. Interfaces* **2013**, *5*, 11392; b) S.-W. Cao, X.-F. Liu, Y.-P. Yuan, Z.-Y. Zhang, Y.-S. Liao, J. Fang, S. C. J. Loo, T. C. Sum, C. Xue, *Appl. Catal. B: Environ.* **2014**, *147*, 940.